An augmented Keller-Segal model for *E. coli* chemotaxis in fast-varying environments

Tong Li* Min Tang† Xu Yang‡

August 26, 2015

Abstract

This is a continuous study on *E. coli* chemotaxis under the framework of pathway-based mean-field theory (PBMFT) proposed in [G. Si, M. Tang and X. Yang, *Multiscale Model. Simul.*, 12 (2014), 907–926], following the physical studies in [G. Si, T. Wu, Q. Quyang and Y. Tu, *Phys. Rev. Lett.*, 109 (2012), 048101]. In this paper, we derive an augmented Keller-Segel system with macroscopic intercellular signaling pathway dynamics. It can explain the experimental observation of phase-shift between the maxima of ligand concentration and density of *E. coli* in fast-varying environments at the population level. This is a necessary complement to the original PBMFT where the phase-shift can only be modeled by moment systems. Formal analysis are given for the system in the cases of fast and slow adaption rates. Numerical simulations show the quantitative agreement of the augmented Keller-Segel model with the individual-based *E. coli* chemotaxis simulator.

1 Introduction

Bacterial chemotaxis has been modeled by the Keller-Segel (K-S) equations at the population level in literature [7], where the drift velocity is given by the empirical functions of the chemoeffector gradient. Modern experimental technologies can now quantitatively measure the dynamics of signaling pathways of *E. coli* ([1, 2, 15, 12]), leading to successful models of internal pathway dynamics [8, 9, 16]. These works provided possibilities of developing predictive agent-based models with the consideration of intracellular signaling pathway dynamics.

In order to connect the microscopic agent-based models to the macroscopic population level K-S model, run-and-tumble kinetic chemotaxis models are introduced, where the tumbling frequency is heuristically depending on the chemical gradient [10]. In the pioneering work of [3, 4, 17], the authors derived macroscopic K-S type models by studying the kinetic chemotaxis models incorporating linear models for signaling pathways. In [14, 13], the authors incorporated the most recent quantitatively measured signaling pathway and recovered the logarithmic sensing property in the K-S model. The connection of these two classes of kinetic models, with and without the signaling pathways, is revealed in [11], which indicates the influence of the molecular content.

*Department of Mathematics University of Iowa Iowa City, 52242 USA. Email: tong-li@uiowa.edu

†Institute of natural sciences and department of mathematics, Shanghai Jiao Tong University, Shanghai, 200240, China. Email: tangmin@sjtu.edu.cn. M.T. was partially supported by NSF of Shanghai under grant 12ZR1445400, NSFC 11301336 and 91330203, and Shanghai Pujiang Program 13PJ140700.

‡Department of Mathematics, University of California, Santa Barbara, CA 93106. Email: xuyang@math.ucsb.edu. X.Y. was partially supported by the NSF grant DMS-1418936 and DMS-1107291: NSF Research Network in Mathematical Sciences "KI-Net: Kinetic description of emerging challenges in multiscale problems of natural science", and Hellman Family Foundation Faculty Fellowship, UC Santa Barbara

Although both types of kinetic models yield the macroscopic K-S model, when the signaling pathways are taken into account, a pathway-based mean field theory (PBMFT) [14, 13] is introduced that can explain a counter-intuitive experimental observation that in a spatial-temporal fast-varying environment, there exists a phase shift between the maxima of ligand concentration and *E. coli* density [18]. Especially, when the time scale of ligand concentration is comparable to the adaptation time scale of *E. coli*, the phase shift becomes significant. This is a phenomenon that cannot be explained by the K-S model [14, 13].

In this paper, we start from the pathway-based mean-field moment system on *E. coli* chemotaxis proposed in [13], and develop an augmented K-S model that can explain the phase shift of *E. coli* dynamics happening in fast-varying environments. The derivation is based on non-dimensionalizing the moment system and noticing that the time scale of average methylation level dynamics is the same as the one of environment variance. The augmented K-S equation is composed by an equation for the bacteria density ρ (1.1a) whose drift velocity and diffusion coefficient are determined by the macroscopic average methylation level M and an additional dynamic equation for M (1.1b):

$$\frac{\partial \rho}{\partial t} = v_0^2 \frac{\partial}{\partial x}\left(Z^{-1} \frac{\partial \rho}{\partial x} \right) - v_0^2 \frac{\partial}{\partial x}\left(Z^{-2} \frac{\partial Z}{\partial m} \frac{\partial M}{\partial x} \rho \right); \tag{1.1a}$$

$$\frac{\partial M}{\partial t} = \kappa F. \tag{1.1b}$$

Here v_0 is the individual running speed of *E. coli*, κ *is the ratio of environmental varying time scale over the one for methylation adaptation.* $Z = z\big(a(M,[L])\big)$, $F = f\big(a(M,[L])\big)$ are two functions depending on the intracellular methylation level M and the extracellular chemoattractant concentration $[L]$. At the microscopic level, they describe the tumbling frequency and the intracellular adaptation dynamics respectively. Their choice in [14, 13] relies on recent measurement in [2, 12]

$$F\big(a(M,[L])\big) = k_R(1 - a/a_0), \qquad Z\big(a(M,[L])\big) = z_0 + \tau^{-1}\big(\frac{a}{a_0}\big)^H, \tag{1.2}$$

where the parameter k_R is the methylation rate, a_0 is the receptor preferred activity, and z_0, H, τ represent the rotational diffusion, the Hill coefficient of flagellar motors response curve and the average run time respectively. The receptor activity $a(M,[L])$ is

$$a = \big(1+\exp(NE)\big)^{-1}, \qquad \text{with } E = -\alpha(M-m_0) + f_0([L]) = -\alpha(M-m_0) + \ln\left(\frac{1+[L]/K_I}{1+[L]/K_A}\right), \tag{1.3}$$

where N, m_0, K_I, K_A represent the number of tightly coupled receptors, basic methylation level, and dissociation constant for inactive receptors and active receptors respectively.

The equation (1.1) can be formally understood as a K-S equation that incorporate intracellular chemo-sensory dynamics. It takes into account the fact that, in fast-varying environment, the environment changes at the time scale of adaptation, and not all E.colis are fully adapted to the change of the environment. Compared to the BPMFT in [14, 13], the augmented K-S model has the advantage of being easily solved and analyzed. We also remark that when the environment changes slowly, κ is large, and thus $F \approx 0$ and $M \approx m_0 + f_0([L])/\alpha$, and (1.1) becomes the standard K-S equation. Numerical results are presented to show the quantitative agreement of the augmented K-S model with the individual-based *E. coli* chemotaxis simulator (SPECS, [5]) in both slow and fast varying environment.

The rest of the paper is organized as follows: We derive the augmented K-S model in Section 2. In Section 3, we analyze the system at the cases of fast and slow adaptive rates, and give some formal

understandings of the system. In Section 4, we verify its validity by numerical comparison to SPECS. Conclusive remarks are made in Section 5.

2 Derivation of the augmented Keller-Segel model

We first summarize the pathway-based mean-field moment system on *E. coli* chemotaxis proposed in [13] for convenience. Under the assumption that the methylation levels of right (left) oriented E.colis are locally concentrated near their average $M^{\pm}$, the moment system can be derived from the kinetic model that incorporate one single additional variable m which represents the intracellular methylation level. Denote the right (left)-traveling densities: $\int p^+ \,\mathrm{d}m$ and the right (left)-oriented moments of methylation m: $\int mp^+ \,\mathrm{d}m$ as ρ^+ (ρ^-) and q^+ (q^-) respectively. They satisfy the following four-equation hyperbolic system:

$$\frac{\partial \rho^+}{\partial t} = -v_0 \frac{\partial \rho^+}{\partial x} - \frac{1}{2}\Big(Z^+\rho^+ - Z^-\rho^-\Big), \tag{2.1a}$$

$$\frac{\partial \rho^-}{\partial t} = v_0 \frac{\partial \rho^-}{\partial x} + \frac{1}{2}\Big(Z^+\rho^+ - Z^-\rho^-\Big), \tag{2.1b}$$

$$\frac{\partial q^+}{\partial t} = -v_0 \frac{\partial q^+}{\partial x} + F^+\rho^+ - \frac{1}{2}\Big(Z^+q^+ - Z^-q^-\Big), \tag{2.1c}$$

$$\frac{\partial q^-}{\partial t} = v_0 \frac{\partial q^-}{\partial x} + F^-\rho^- + \frac{1}{2}\Big(Z^+q^+ - Z^-q^-\Big). \tag{2.1d}$$

Here $M^{\pm} = q^{\pm}/\rho^{\pm}$ is the right (left) oriented average methylation level, and $F^{\pm} = F\big(a(M^{\pm}, [L])\big)$, $Z^{\pm} = Z\big(a(M^{\pm}, [L])\big)$.

We nondimensionalize (2.1) by

$$t = T\tilde{t}, \qquad x = L\tilde{x}, \qquad v_0 = s_0\tilde{v}_0,$$

where T, L are temporal and spatial scales of the *E. coli* system respectively. Then (2.1) becomes, after dropping the "$\sim$",

$$\frac{1}{T}\frac{\partial \rho^+}{\partial t} = -\frac{s_0}{L} v_0 \frac{\partial \rho^+}{\partial x} - \frac{1}{2T_1}\Big(Z^+\rho^+ - Z^-\rho^-\Big), \tag{2.2a}$$

$$\frac{1}{T}\frac{\partial \rho^-}{\partial t} = \frac{s_0}{L} v_0 \frac{\partial \rho^-}{\partial x} + \frac{1}{2T_1}\Big(Z^+\rho^+ - Z^-\rho^-\Big), \tag{2.2b}$$

$$\begin{aligned}\frac{1}{T_f}\rho^+\frac{\partial M^+}{\partial t} + \frac{1}{T}M^+\frac{\partial \rho^+}{\partial t} = &-\frac{s_0}{L} v_0 \frac{\partial q^+}{\partial x} \\ &+ \frac{1}{T_2}F^+\rho^+ - \frac{1}{2T_1}\Big(Z^+q^+ - Z^-q^-\Big),\end{aligned} \tag{2.2c}$$

$$\begin{aligned}\frac{1}{T_f}\rho^-\frac{\partial M^-}{\partial t} + \frac{1}{T}M^-\frac{\partial \rho^-}{\partial t} = &\frac{s_0}{L} v_0 \frac{\partial q^-}{\partial x} \\ &+ \frac{1}{T_2}F^-\rho^- + \frac{1}{2T_1}\Big(Z^+q^+ - Z^-q^-\Big),\end{aligned} \tag{2.2d}$$

where T_1, T_2 are the average run and signaling adaptation time scales respectively and T_f is the time scale that the macroscopic methylation level changes which the same as the time scale that the environment varies.

For *E. coli* chemotaixs, the average run time is at the order of 1s, the signaling adaptation time is approximately $10s \sim 100$s, and the observation system time scale is about 1000s. It is reasonable to consider the long time regime, where the tumbling frequency becomes large (the so-called parabolic scaling). The main difference from the derivation of the standard K-S equation is that we separate out the scale T_f, whose scale is the same as the variation of the environment. We consider the following scaling

$$\frac{T_1}{L/s_0} = \varepsilon, \quad \frac{T_2}{L/s_0} = 1, \quad \frac{T}{L/s_0} = \frac{1}{\varepsilon}, \quad \text{and} \quad \frac{T_f}{L/s_0} = \frac{1}{\kappa}, \tag{2.3}$$

where ϵ is small. Since T_f ranges from $100s$ to $800s$ in the experiment in [18], κ ranges from $O(\epsilon)$ to $O(1)$. Then (2.2) becomes

$$\varepsilon\frac{\partial \rho^+}{\partial t} = -v_0\frac{\partial \rho^+}{\partial x} - \frac{1}{2\varepsilon}\Big(Z^+\rho^+ - Z^-\rho^-\Big), \tag{2.4a}$$

$$\varepsilon\frac{\partial \rho^-}{\partial t} = v_0\frac{\partial \rho^-}{\partial x} + \frac{1}{2\varepsilon}\Big(Z^+\rho^+ - Z^-\rho^-\Big), \tag{2.4b}$$

$$\kappa\rho^+\frac{\partial M^+}{\partial t} + \varepsilon M^+\frac{\partial \rho^+}{\partial t} = -v_0\frac{\partial q^+}{\partial x} + F^+\rho^+ - \frac{1}{2\varepsilon}\Big(M^+Z^+\rho^+ - M^-Z^-\rho^-\Big), \tag{2.4c}$$

$$\kappa\rho^-\frac{\partial M^-}{\partial t} + \varepsilon M^-\frac{\partial \rho^-}{\partial t} = v_0\frac{\partial q^-}{\partial x} + F^-\rho^- + \frac{1}{2\varepsilon}\Big(M^+Z^+\rho^+ - M^-Z^-\rho^-\Big). \tag{2.4d}$$

We consider the following asymptotic expansion

$$\rho^\pm = \rho^{\pm(0)} + \varepsilon\rho^{\pm(1)} + \cdots, \qquad q^\pm = q^{\pm(0)} + \varepsilon q^{\pm(1)} + \cdots, \qquad M^\pm = M^{\pm(0)} + \varepsilon M^{\pm(1)} + \cdots,$$
$$F^\pm = F^{\pm(0)} + \varepsilon F^{\pm(1)} + \cdots, \quad Z^\pm = Z^{\pm(0)} + \varepsilon Z^{\pm(1)} + \cdots.$$

Matching the $O(1/\varepsilon)$ terms in (2.4a) and (2.4c) yields

$$Z^{+(0)}\rho^{+(0)} = Z^{-(0)}\rho^{-(0)} \quad \text{and} \quad M^{+(0)}Z^{+(0)}\rho^{+(0)} = M^{-(0)}Z^{-(0)}\rho^{-(0)},$$

which gives

$$M^{+(0)} = M^{-(0)} = M_0,\ Z^{+(0)} = Z^{-(0)} = Z_0,\ F^{+(0)} = F^{-(0)} = F_0;$$
$$\rho^{+(0)} = \rho^{-(0)} = \rho_0,\ q^{+(0)} = q^{-(0)} = q_0.$$

The $O(1)$ terms in the sum of (2.4c) and (2.4d) yield

$$\kappa\frac{\partial M_0}{\partial t} = F_0. \tag{2.5}$$

Since $F_0 = k_R\big(1 - a(M_0)/a_0\big)$,

$$\frac{\partial M_0}{\partial t} = \frac{k_R}{\kappa}\big(1 - a(M_0)/a_0\big). \tag{2.6}$$

Equating the $O(\varepsilon)$ terms in the sum of (2.4a) and (2.4b) produces

$$\frac{\partial \rho_0}{\partial t} = -v_0\frac{\partial(\rho^{+(1)} - \rho^{-(1)})}{2\partial x}. \tag{2.7}$$

Together with (2.5), the $O(1)$ terms in (2.4a)-(2.4b) and (2.4c)-(2.4d) bring

$$2v_0\frac{\partial \rho_0}{\partial x} + Z_0(\rho^{+(1)} - \rho^{-(1)}) + \rho_0(Z^{+(1)} - Z^{-(1)}) = 0, \tag{2.8}$$

$$2v_0\frac{\partial q_0}{\partial x} + \rho_0 M_0(Z^{+(1)} - Z^{-(1)}) + \rho_0 Z_0(M^{+(1)} - M^{-(1)}) + M_0 Z_0(\rho^{+(1)} - \rho^{-(1)}) = 0. \tag{2.9}$$

Multiplying (2.8) by M_0 and subtracting it from (2.9) yield

$$2v_0\rho_0\frac{\partial M_0}{\partial x} + \rho_0 Z_0(M^{+(1)} - M^{-(1)}) = 0.$$

Denoting $\frac{\partial z}{\partial m}\big|_{m=M_0} = \frac{\partial Z_0}{\partial m}$, then by

$$Z^{\pm} = z(M^{\pm}) = z\big(M_0 + \varepsilon M^{\pm(1)} + \cdots\big) = Z_0 + \varepsilon\frac{\partial Z_0}{\partial m}M^{\pm(1)} + \cdots,$$

one has $Z^{+(1)} - Z^{-(1)} = \frac{\partial Z_0}{\partial m}\big(M^{+(1)} - M^{-(1)}\big)$. Therefore, (2.8) indicates

$$\begin{aligned}\rho^{+(1)} - \rho^{-(1)} &= -2v_0 Z_0^{-1}\frac{\partial \rho_0}{\partial x} - \rho_0 Z_0^{-1}\frac{\partial Z_0}{\partial m}(M^{+(1)} - M^{-(1)}) \\ &= -2v_0 Z_0^{-1}\frac{\partial \rho_0}{\partial x} + v_0 Z_0^{-2}\frac{\partial Z_0}{\partial m}\frac{\partial M_0}{\partial x}\rho_0.\end{aligned}$$

Substituting the above equation into (2.7) yields the augmented K-S equation

$$\frac{\partial \rho_0}{\partial t} = v_0^2\frac{\partial}{\partial x}\left(Z_0^{-1}\frac{\partial \rho_0}{\partial x}\right) - \frac{v_0^2}{2}\frac{\partial}{\partial x}\left(Z_0^{-2}\frac{\partial Z_0}{\partial m}\frac{\partial M_0}{\partial x}\rho_0\right), \tag{2.10}$$

with M_0 given by (2.6). The dependence on the outside signal is implicitly included in the expression of a, since a is a function of M_0 and $[L]$, (2.6) depends on $[L]$, so are the diffusion and chemo-sensitivity coefficients in (2.10). It can be understood as a K-S equation incorporated with macroscopic dynamics of methylation level whose adaptation rate is given by the ratio of the microscopic adaptation time for each E.coli over the one of environmental variance.

3 Formal understanding

The system (1.1) depends on the environment by the fact that a is a function of both methylation level m and extracellular chemoattractant concentration $[L]$. The complex nonlinear dependence of the coefficients on $[L]$ makes it hard to have an intuitive idea of the population behavior. In order to understand the population behavior, we reformulate (1.1) into a system for the bacteria population density ρ and average activity a.

Let

$$S = \ln\left(\frac{1 + [L]/K_I}{1 + [L]/K_A}\right). \tag{3.1}$$

From (1.3),

$$\frac{\partial a}{\partial M} = N\alpha a(1-a), \qquad \frac{\partial a}{\partial S} = -Na(1-a),$$

together with (2.6) and

$$\frac{\partial Z}{\partial M}=\frac{\partial Z}{\partial a}\frac{\partial a}{\partial M},\qquad \frac{\partial a}{\partial x}=\frac{\partial a}{\partial M}\frac{\partial M}{\partial x}+\frac{\partial a}{\partial S}\frac{\partial S}{\partial x},\qquad \frac{\partial a}{\partial t}=\frac{\partial a}{\partial M}\frac{\partial M}{\partial t}+\frac{\partial a}{\partial S}\frac{\partial S}{\partial t},$$

we find

$$Z^{-2}\frac{\partial Z}{\partial M}\frac{\partial M}{\partial x}=Z^{-2}\frac{\partial Z}{\partial a}\Big(\frac{\partial a}{\partial x}+Na(1-a)\frac{\partial S}{\partial x}\Big),\qquad \frac{\partial a}{\partial t}=\frac{k_R}{\kappa}\frac{\partial a}{\partial M}(1-a/a_0)-Na(1-a)\frac{\partial S}{\partial t}.$$

Therefore, the system (1.1) can be written into a system for ρ and a such that

$$\frac{\partial \rho}{\partial t}=v_0^2\frac{\partial}{\partial x}\bigg(Z^{-1}\frac{\partial \rho}{\partial x}\bigg)-\frac{v_0^2}{2}\frac{\partial}{\partial x}\bigg(Z^{-2}\frac{\partial Z}{\partial a}Na(1-a)\frac{\partial S}{\partial x}\rho\bigg)-\frac{v_0^2}{2}\frac{\partial}{\partial x}\bigg(Z^{-2}\frac{\partial Z}{\partial a}\frac{\partial a}{\partial x}\rho\bigg),\tag{3.2a}$$

$$\frac{\partial a}{\partial t}=\frac{k_R}{\kappa}N\alpha a(1-a)(1-a/a_0)-Na(1-a)\frac{\partial S}{\partial t}.\tag{3.2b}$$

In (3.2), the first two terms on the right hand side of the equation for ρ is the same as the standard K-S model. Particularly, since $0<a_0<1$, the first term on the right hand side of the equation for a has the effect that let a converge to a_0. when the environment changes slow comparing to the adaptation time, i.e. k_R/κ is large, the first term on the right hand side of (3.2b) dominates, $a\approx a_0$ and the last term in (3.2a) for ρ vanishes. The population behavior of (3.2) is the same as the standard K-S model.

The last terms on the right-hand side of (3.2) take into account the fast variation in time. We introduce $\eta=\frac{\kappa}{k_RN\alpha}$, and rewrite (3.2b) as

$$\frac{\partial a}{\partial t}=\frac{1}{\eta}a(1-a)\big(1-a/a_0-N\eta\frac{\partial S}{\partial t}\big).\tag{3.3}$$

Proposition 3.1 *For the system*

$$\frac{\partial \rho}{\partial t}=v_0^2\frac{\partial}{\partial x}\bigg(D(a)\frac{\partial \rho}{\partial x}\bigg)-\frac{\partial}{\partial x}\bigg(\chi(a)\frac{\partial S}{\partial x}\rho\bigg)-\frac{\partial}{\partial x}\bigg(C(a)\frac{\partial a}{\partial x}\rho\bigg),\tag{3.4a}$$

$$\eta\frac{\partial a}{\partial t}=a(1-a)\big(1-a/a_0-N\eta\frac{\partial S}{\partial t}\big),\tag{3.4b}$$

with $D(a)$, $\chi(a)$ and $C(a)$ some positive decreasing functions in a. When $\eta\to 0$, $a=a_0$ is the unique stable steady state for (3.4b)*. Assume $|\partial_t S|$ is bounded,* (3.4) *converges to the K-S equation. When $\partial_t S>\delta$ (δ is some positive constant) and η large, the stable steady state is $a=0$ while the stable steady state switches to $a=1$ when $\partial_t S<-\delta$.*

Proof. The proof is straight forward. When $\eta\to 0$, the limit equation for a is

$$\frac{\partial a}{\partial t}=\frac{1}{\eta}a(1-a)\big(1-a/a_0\big),$$

it has three steady solutions, $a=0,a_0,1$, but only a_0 is stable, which implies that $a\to a_0$ as $t\to+\infty$. This yields the standard KS equation. When $\eta\to+\infty$, (3.4b) becomes

$$\frac{\partial a}{\partial t}=a(1-a)\partial_t S.$$

The two steady states are $a = 0, 1$. When $\partial_t S > \delta > 0$, only $a = 0$ is stable while when $\partial_t S < -\delta < 0$, $a = 1$ is stable. $\square$

Therefore, in the intermediate regime, when $\partial_t S > 0$, $0 < a < a_0$, while when $\partial_t S < 0$, $a_0 < a < 1$. This can be verified in the numerical simulations as in section 4.

For $\eta << 1$, if we consider the asymptotic expansions with respect to η, the first two terms on the right-hand side of (3.3) is $a_0 - \eta a_0 N \partial_t S$. Then, the equation for ρ becomes

$$\begin{aligned}\frac{\partial \rho}{\partial t} =& v_0^2 \frac{\partial}{\partial x}\left(Z_0^{-1}\frac{\partial \rho}{\partial x}\right) - \frac{v_0^2}{2}\frac{\partial}{\partial x}\left(Z_0^{-2}\frac{\partial Z_0}{\partial a}Na_0(1-a_0)\frac{\partial S}{\partial x}\rho\right) + \frac{1}{2}\eta a_0 N v_0^2 \frac{\partial}{\partial x}\left(Z_0^{-2}\frac{\partial Z_0}{\partial a}\frac{\partial^2 S}{\partial t \partial x}\rho\right), \\ &+ \eta a_0 N v_0^2 \frac{\partial}{\partial x}\left(Z_0^{-2}\frac{\partial Z_0}{\partial a}\frac{\partial S}{\partial t}\frac{\partial \rho}{\partial x}\right) + \frac{1}{2}\eta a_0 N v_0^2 \frac{\partial}{\partial x}\left(\frac{\partial\left(Z_0^{-2}\frac{\partial Z_0}{\partial a}Na_0(1-a_0)\right)}{\partial a}\frac{\partial S}{\partial t}\frac{\partial S}{\partial x}\rho\right)\end{aligned} \tag{3.5}$$

This is a modified KS model with $\partial_t S$ dependent advection and diffusion. The equation looks complex, but all coefficients are constants, except S being determined by the outside signal. This linearized version is not well-posed when S decreases fast, however, it provides the intuition that the diffusion and advection coefficients depends on $\partial_t S$ instead of S itself. This is an important observation, since at the cell level, bacteria can "feel" S while at the population level, only $\partial_x S$ or $\partial_t S$.

Remark 3.2 *Since the biologically measurable parameters $K_A >> K_I$, when $K_I << [L] << K_A$, $S \approx \chi \ln[L]$, we can simplify* (3.5) *further by replacing S by $\ln[L]$. In the limit $\eta \to 0$, this yields the spacial logarithm sensitivity of E.coli chemotaxis, which have been proved experimentally [6].* (3.5) *indicates the temporal logarithm sensitivity.*

4 Numerical Results

We show the numerical comparison of SPECS to the augmented K-S model in this section. SPECS is a cell based microscopic model that takes into account the evolution of each cell intracellular methylation level by $\partial_t m = F(a(m, [L]))$. It is easy to run a Monte Carlo simulation with particles whose tumbling frequency of each bacteria is determined by $Z(a(m, [L]))$ in (1.2). SPECS and the kinetic model with an incorporation of intracellular chemo-sensory systems showed a quantitative match in [14, 13]. They can both capture the behavior *E. coli* chemotaxis at the population level in fast varying environments.

Following the setup in [13, 14], we choose a periodic one-dimensional traveling wave concentration $[L](x,t) = [L]_0 + [L]_A \sin[\frac{2\pi}{\lambda}(x - ut)]$ environment to show how the intracellular signaling dynamics affects the behavior of *E. coli* at the population level. Here the environment is spatial-temporal varying and the wavelength λ is the length of the domain. The advantage of the periodic environment set up is that it is experimentally realizable and u is experimentally tunable.

We compare the densities ρ and the macroscopic activities $a(M_0)$ in Figure 1. The density is scaled at the order of 10^{-3}. In SPECS, the density is defined as the ratio of the actual *E. coli* number in a cell over the total number, and the macroscopic activity $a(M)$ is defined as the average of all *E. coli* activities in a cell. For different choices traveling wave velocities $u = 0.4\mu m/s$ and $u = 8\mu m/s$, quantitatively consistency can be observed for the results of SPECS and the augmented K-S model. In Figure 1, the x axis represents the remainder of $x - ut \bmod \ell$, *i.e.* we keep tracking the wave front of the periodic traveling wave.

When the environment changes slowly (*i.e.* $u = 0.4\mu m/s$), $a(M)$ is close to a_0, indicating that the methylation levels of most *E.colis* have been fully relaxed to the stationary state, while in the fast-varying environment (*i.e.* $u = 8\mu m/s$), $a(M)$ is away from a_0, due to the slow signaling adaptation

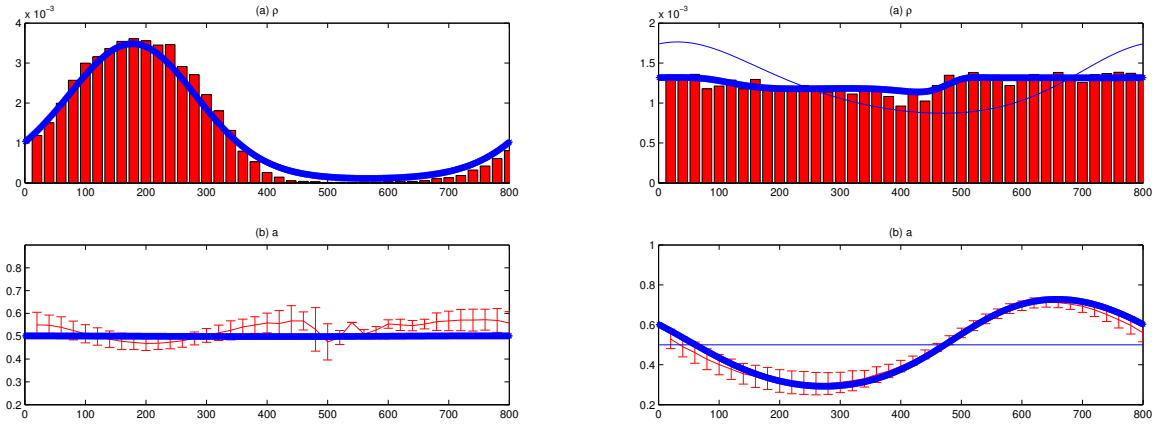

Figure 1: Numerical comparison of the augmented K-S model to SPECS [5]. The steady state profiles of ρ (top) and $a(M)$ (bottom) are presented. Left: $u = 0.4\mu m/s$; Right: $u = 8\mu m/s$. In the subfigures, histograms and dots are from SPECS, solid lines are from the classical K-S equation while dash-star lines are calculated using the augmented K-S model. The solid lines can not be seen in the left subfigures since they are overlapped with the dashed-star lines. Parameters for the environment used here are $[L]_0 = 500\mu M$, $[L]_A = 100\mu M$, $\lambda = 800\mu m$. Parameters for E.coli chemotaxis are $\alpha = 1.7$, $m_0 = 1$, $K_I = 18.2\mu M$, $K_A = 3mM$, $N = 6$, $k_R = 0.01s^{-1}$, $a_0 = 0.5$, $z_0 = 0.14s^{-1}$, $\tau = 0.8s$, $H = 10$. 20000 cells are simulated in SPECS.

rate. This difference leads to the difference in the profiles of ρ that when $u = 0.4\mu m/s$, the bacteria density is larger at where the concentration $[L]$ is larger, while the case of $u = 8\mu m/s$ indicates the phase-shift between the density and concentration profiles. More physical explanations are referred to [5, 14].

Furthermore, the comparison of the three different KS models are displayed in Figure 2, we can see the difference in the population level behavior even in slow varying environment. The model (3.5) is no longer right when u becomes large.

5 Conclusion

In this paper, we propose an augmented Keller-Segel model for the population dynamics of *E. coli* in the fast-varying environments. The model is derived by rescaling the moment system proposed in [13] under the assumption that the time scale of methylation level variation is comparable to the dynamics of the environment. Numerical verification is provided by comparison to the individual-based *E. coli* chemotaxis simulator [5]. The phase-shift between the maxima of ligand concentration and density of *E. coli* in fast-varying environments can be observed, and thus makes it a necessary complement to the original PBMFT where the phase-shift can only be modeled by moment systems.

We would like to emphasis that all functions and parameters used in the model derivation and numerical experiments are biologically measurable. The major interest of this paper is not only the model derivation but also its applicability to real experimental predictions.

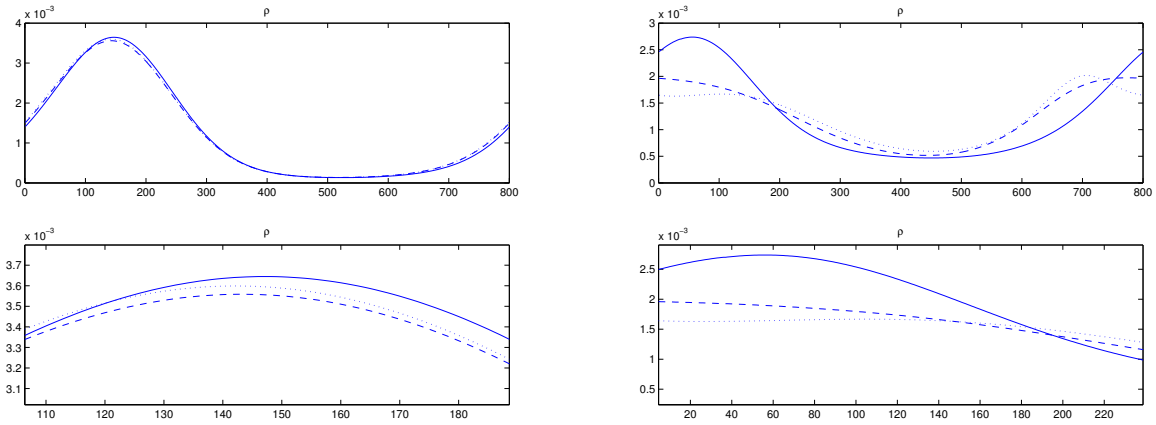

Figure 2: The difference between the three different KS models are presented. The spacial temporal varying environment evolves according to $[L](x,t) = [L]_0 + [L]_A \sin[\frac{2\pi}{\lambda}(x-ut)]$. Solid lines, dashed and dash-dotted lines are respectively from the classical KS equation, the modified KS equation coupled with an ODE (2.10) (2.6) and the modified KS equation taking into account the time derivatives of the chemical signal (3.5). Left: $u = 0.8\mu m/s$; Right: $u = 2\mu m/s$. The bottom subplots are the zoom in of the top subplots. All parameters are the same as Figure 2.

References

[1] U. Alon, M.G. Surette, N. Barkai, and S. Leibler, *Robustness in bacterial chemotaxis*, Nature **397** (1999), 168–171.

[2] P. Cluzel, M. Surette, and S. Leibler, *An ultrasensitive bacterial motor revealed by monitoring signalling proteins in single cells*, Science **287** (2000), 1652–1655.

[3] R. Erban and H.G. Othmer, *From individual to collective behavior in bacterial chemotaxis*, SIAM J. Appl. Math. **65** (2004), 361–391.

[4] _____, *From signal transduction to spatial pattern formation in E. coli: A paradigm for multi-scale modeling in biology*, Multiscale Model. Simul. **3** (2005), 362–394.

[5] L. Jiang, Q. Ouyang, and Y. Tu, *Quantitative modeling of Escherichia coli chemotactic motion in environments varying in space and time*, PLoS Comput. Biol. **6** (2010), e1000735.

[6] Y. V. Kalinin, L. Jiang, Y. Tu and M. Wu, *Logarithmic Sensing in Escherichia coli Bacterial Chemotaxis*, Biophys J. **96(6)** (2009), 24392448.

[7] E. Keller and L. Segel, *Model for chemotaxis*, J. Theor. Biol. **30** (1971), 225–234.

[8] J.E. Keymer, R.G. Endres, M. Skoge, Y. Meir, and N.S. Wingreen, *Chemosensing in escherichia coli: two regimes of two-state receptors*, Proc. Natl. Acad. Sci. U.S.A. **103** (2006), no. 6, 1786.

[9] B.A. Mello and Y. Tu, *Quantitative modeling of sensitivity in bacterial chemotaxis: The role of coupling among different chemoreceptor species*, Proc. Natl. Acad. Sci. **100** (2003), 8223–8228.

[10] H.G. Othmer and T. Hillen, *The diffusion limit of transport equations II: Chemotaxis equations*, SIAM J. Appl. Math. **62** (2002), 1222–1250.

[11] B. Perthame, M. Tang, and N. Vauchelet, *Derivation of the bacterial run-and-tumble kinetic equation from a model with biochemical pathway*, submitted.

[12] T.S. Shimizu, Y. Tu, and H.C. Berg, *A modular gradient-sensing network for chemotaxis in Escherichia coli revealed by responses to time-varying stimuli*, Mol. Syst. Biol. **6** (2010), 382.

[13] G. Si, M. Tang, and X. Yang, *A pathway-based mean-field model for E. coli chemotaxis: Mathematical derivation and its hyperbolic and parabolic limits*, Multiscale Model. Simul. **12** (2014), 907–926.

[14] G. Si, T. Wu, Q. Ouyang, and Y. Tu, *A pathway-based mean-field model for Escherichia coli chemotaxis*, Phys. Rev. Lett. **109** (2012), 048101.

[15] V. Sourjik and H.C. Berg, *Receptor sensitivity in bacterial chemotaxis*, Proc. Natl. Acad. Sci. **99** (2002), 123–127.

[16] Y. Tu, T.S. Shimizu, and H.C. Berg, *Modeling the chemotactic response of escherichia coli to time-varying stimuli*, Proc. Natl. Acad. Sci. U.S.A. **105** (2008), no. 39, 14855.

[17] C. Xue and H.G. Othmer, *Multiscale models of taxis-driven patterning in bacterial pupulaitons*, SIAM J. Appl. Math. **70** (2009), 133–167.

[18] X. Zhu, G. Si, N. Deng, Q. Ouyang, T. Wu, Z. He, L. Jiang, C. Luo, and Y. Tu, *Frequency-dependent Escherichia coli chemotaxis behavior*, Phys. Rev. Lett. **108** (2012), 128101.